JOURNAL OF AIRCRAFT
Vol. 47, No. 5, September–October 2010

Stochastic Modeling of Incident Gust Effects on Aerodynamic Lift

M. Ghommem* and M. R. Hajj†
Virginia Polytechnic Institute and State University, Blacksburg, Virginia 24061
C. L. Pettit‡
United States Naval Academy, Annapolis, Maryland 21402
and
P. S. Beran‡
Air Force Research Laboratory, Wright-Patterson Air Force Base, Ohio 45433-7542

DOI: 10.2514/1.C000257

The intrusive formulation of polynomial chaos expansion is implemented to determine uncertainty in aerodynamic loads on a rigid airfoil due to imprecise parameters that characterize an incoming gust. The results yield the sensitivity of the lift coefficient to variations in intensities and integral length scales of the gust fluctuations. The results show that lift coefficient fluctuations about the mean of each time step are affected primarily by the intensity of the fluctuations of the vertical velocity component, which should be expected. Next in order of importance is the integral length scale of the vertical velocity component. This implementation of the intrusive polynomial chaos expansion provides guidance for future efforts to quantify uncertain gust loads on micro air vehicles with higher fidelity models.

Nomenclature

C_p	=	pressure coefficient
c_l	=	aerodynamic lift
L	=	integral length scale
N	=	number of bound vortices
N_w	=	number of wake vortices
p	=	pressure
$\mathbf{r}$	=	position vector
t	=	time
$\mathbf{V}$	=	velocity
xc	=	control points
xv	=	vortex points
α	=	angle of attack
γ	=	circulation density
Δt	=	time step
Δl	=	panel length
Ξ	=	random vector
ξ	=	random variable
ρ	=	density
σ	=	turbulence intensity
Φ	=	velocity potential
ϕ	=	phase
Ψ	=	random basis function

Subscripts

b	=	bound
c	=	control point
l	=	lower
n	=	normal direction of the plate
te	=	trailing edge
u	=	upper
u	=	horizontal direction
v	=	vertical direction
w	=	wake
∞	=	freestream

Received 12 January 2010; revision received 30 June 2010; accepted for publication 30 June 2010.

*Department of Engineering Science and Mechanics. Student Member AIAA.
†Department of Engineering Science and Mechanics.
‡Member AIAA.

I. Introduction

ASSESSING upstream gust effects on flow quantities is required in many aeroelastic applications. This is particularly important for micro air vehicles (MAV) which are expected to operate in urban environments, where they will be subjected to varying turbulent or gust flows. Under these conditions, a quasi-steady approach would not yield correct aerodynamic forces as its temporal or length scale would be much larger than the ones in the range encountered by MAV. Consequently, upstream gust or turbulence should be modeled through many parameters, including turbulence intensities, integral length scales, relative energy content of large and small scales, and the aerodynamic roughness in the case of boundary layers. These parameters may not be known precisely or accurately. This is because they are statistics of flow quantities whose sampling distributions cannot be easily known a priori for the complex terrains in which MAVs are expected to operate. Furthermore, because these parameters cannot be changed independently [1], it is difficult to perform a parametric assessment of their individual effects on different flow quantities [2,3].

The influence of the likely range of gust statistics on unsteady aerodynamic loads can best be quantified through a broad sensitivity analysis. Comprehensive sampling-based simulations that make use of blind or wide variations of input parameters are inefficient for aeroelastic simulations which are already computationally expensive, even in the deterministic sense. As such, an integrated approach that enables uncertainty propagation through the model would be more effective for performing sensitivity analysis of flow quantities to ranges of gust or turbulence parameters. The central role of sensitivity analysis in support of uncertainty quantification (UQ) is broadly recognized [4,5]. Formal uncertainty quantification (UQ) of unsteady aerodynamics and aeroelasticity has been an active area of research for at least the past 15 years. Pettit [6] summarized various UQ perspectives and methods in the context of aeroelasticity and surveyed the state of the field through 2004. Among the methods

Pettit surveyed, series expansions of stochastic processes in terms of orthogonal functions of random variables were cited for their potential to integrate UQ with standard computational methods.

In this study, the intrusive formulation of the polynomial chaos expansion (PCE) is implemented to quantify the influence of imprecision in upstream gust parameters on aerodynamic loads on a rigid airfoil. This formulation involves the substitution of uncertain variables and parameters in the governing equations with polynomial expansions. The unknown polynomial coefficients are then evaluated by projecting the resulting equations onto basis functions. Thus, the governing equations are reformulated to yield mode strengths [7] of the output, which in this case is the unsteady lift coefficient. The aerodynamic model used in this effort is based on the unsteady vortex lattice method (UVLM). This relatively simple method, with linear assumptions, is chosen as a first step to determine whether the PCE approach can be implemented in a nonlinear formulation of the deterministic problem, e.g., if the flow is modeled by Euler or Navier–Stokes equations.

II. Stochastic Gust Representation

Typically, turbulent fluctuations of the different velocity components of a flow field are compactly specified by frequency-domain power spectra [8,9] such as the von Karman spectrum [10,11]. In this representation, the spectra of the velocity components are given by [11]

$$S_{uu}(\omega) = \frac{2\sigma_u^2 L_u}{\pi V_\infty} \frac{1}{[1 + (1.339 L_u \omega / V_\infty)^2]^{5/6}}$$
$$S_{vv}(\omega) = \frac{2\sigma_v^2 L_v}{\pi V_\infty} \frac{1 + \frac{8}{3}(2.678 L_v \omega / V_\infty)^2}{[1 + (2.678 L_v \omega / V_\infty)^2]^{11/6}} \tag{1}$$

where L_u and L_v, are, respectively, the integral length scales of the horizontal and vertical velocity fluctuations, and σ_u and σ_v, are used to denote the corresponding turbulence intensities.

In this work, stochastic gust fluctuations are obtained by superposing a finite set of sinusoidal components defined from their corresponding power spectra as follows

$$u(t) = \sum_{n=1}^{N_\omega} \sqrt{2 S_{uu}(\omega_n) \Delta\omega_n(\omega_n)} \cos(\omega_n t + \phi_n) \quad \text{and}$$
$$v(t) = \sum_{n=1}^{N_\omega} \sqrt{2 S_{vv}(\omega_n) \Delta\omega_n(\omega_n)} \cos(\omega_n t + \phi_n) \tag{2}$$

where the phase ϕ_n corresponding to each frequency component is a uniform random variable between 0 and 2π. It should be noted that for a particular group of spectral parameters, choosing a different set of phases ϕ_n will produce a different time history, but with the same long-term statistics because these are governed by the particular spectrum. In effect, this would introduce an additional N_ω random variables in the time integration problem that are not present in the frequency domain [12]. These variables are not part of the random parameters considered in the subsequent analysis. Consequently, the set of phases ϕ_n is kept the same for all realizations. Additional details of the approach followed to represent fluctuations in atmospheric flows are provided by Paola [13] and Grigoriu [14].

III. UVLM Implementation

A. Formulation

The time-varying flow around the flat-plate airfoil is modeled using a two-dimensional UVLM. This method has been used extensively to determine aerodynamic loads and aeroelastic responses by [15,16]. Highlights of this method are detailed below to show how the intrusive PCE can be conveniently implemented when using UVLM.

The position of the wake and the distribution of circulation on the plate and in the wake are treated as unknowns. The plate is divided into N piecewise straight line segments or panels. In each panel, a point vortex with a circulation density $(\gamma_b)_i(t)$ is placed at the one-quarter chord position. The no-penetration condition is imposed at the three-quarter chord position, called the control point. Figure 1 shows a schematic of the flat plate with panels, each of them having a concentrated vortex located at $xv(i)$, and a control point located at $xc(i)$.

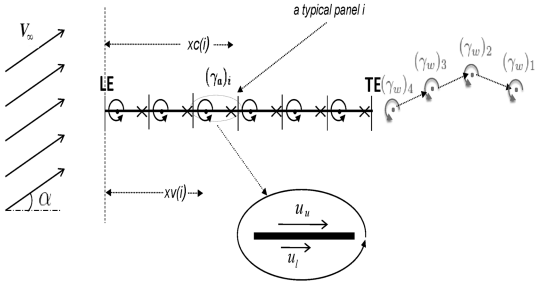

Fig. 1 Representation of a model of a flat plate with panels, each one has a concentrated vortex located at $xv(i)$, and a control point located at $xc(i)$.

The time-varying gust is denoted by $\mathbf{V}_\infty(t) = [V_\infty + u(t), v(t)]^T$ and is introduced in the UVLM representation. The basic mathematical tool in this method is the expression derived from the Biot-Savart law that gives the velocity $\mathbf{V}$ at a point $\mathbf{r}$ associated with an individual vortex point located at $\mathbf{r}_0$ and having circulation $\gamma(t)$; that is,

$$\mathbf{V}(\mathbf{r}, t) = -\frac{1}{2\pi} \mathbf{e}_z \times \gamma(t) \frac{\mathbf{r} - \mathbf{r}_0}{|\mathbf{r} - \mathbf{r}_0|^2} \tag{3}$$

where $\mathbf{e}_z$ is a unit vector perpendicular to the (x, y) plane so as to form a right-hand system with the basis vectors in the plane of the flow. Consequently, the normal component of the velocity at the control point of panel i, $xc(i)$, associated with the flow around the vortex in panel j, $xv(j)$, is

$$\mathbf{u}_b(i, j) \cdot \mathbf{n} = u_{b_n}(i, j) = \frac{(\gamma_b)_j(t)}{2\pi} \left[\frac{1}{xv(j) - xc(i)} \right]$$
$$= (\gamma_b)_j(t) L_1(i, j) \tag{4}$$

where $\mathbf{n}$ is the normal vector of the plate. The operator L_1 is used to denote the induced velocity obtained from the Biot–Savart law. The total normal component of the velocity at control point i attributed to the disturbance created by all bound vortices is then given by

$$u_{b_n}(i)|_{\text{total}} = \sum_{j=1}^{N} u_{b_n}(i, j) = \sum_{j=1}^{N} (\gamma_b)_j(t) L_1(i, j) \tag{5}$$

B. Wake Development

The wake vorticity is introduced by shedding point vortices from the trailing edge, whose circulation is denoted by $(\gamma_w)_j(t)$. These vortices are convected downstream at each time step and their positions are denoted by $(\mathbf{r}_w)_j(t)$. The induced velocity at control point i that stems from all wake vortices is given by

$$\mathbf{u}_w(i) = -\frac{1}{2\pi} \mathbf{e}_z \times \sum_{j=1}^{N_w(t)} (\gamma_w)_j(t) \frac{\mathbf{r}_{c_i} - (\mathbf{r}_w)_j}{|\mathbf{r}_{c_i} - (\mathbf{r}_w)_j|^2} \tag{6}$$

where $\mathbf{r}_{c_i}$ is the position of the control point i in the global frame and $N_w(t)$ is the number of wake vortices. Additionally, there is the normal component of the freestream velocity, which, in this case, is the same for all control points $\mathbf{V}_\infty(t) \cdot \mathbf{n} = -L_3 \mathbf{V}_\infty(t)$.

At every control point, the no-penetration condition applies and is written in the form

$$u_{b_n} = (-\mathbf{u}_w - \mathbf{V}_\infty) \cdot \mathbf{n} \tag{7}$$

In terms $\gamma_b(t)$, $\mathbf{r}_w(t)$, and $\gamma_w(t)$, this condition is written as

$$L_1 \gamma_b(t) = L_2(\mathbf{r}_w(t)) \gamma_w(t) + L_3 \mathbf{V}_\infty(t) \tag{8}$$

where L_2 denotes a geometric operator that represents the induced velocity obtained form the Biot-Savart law and L_3 is an operator through which the fluctuations in the freestream velocity impact each control point.

At every time step, a vortex with circulation γ_{te} is shed from the trailing edge of the plate into the wake. The conservation of the total circulation yields

$$\sum_{i=1}^{N}(\gamma_b)_i(t) + \gamma_{te}(t) = -\sum_{j=1}^{N_w(t)}(\gamma_w)_j(t) \tag{9}$$

It is noted that vortices shed from the trailing edge retain their circulation values at all times. Thereafter, solving Eq. (9) for given $(\gamma_b)_i(t)$ and $(\gamma_w)_j(t)$, and updating the vector of wake vortices yields

$$(\gamma_w)_1(t+1) = \gamma_{te}(t) \tag{10}$$

and

$$(\gamma_w)_{i+1}(t+1) = (\gamma_w)_i(t), \quad \text{for } i = 1, 2, \ldots, N_w(t) \tag{11}$$

The steps described in Eqs. (9–11) are then summarized as:

$$\gamma_w(t+1) = L_4\gamma_w(t) + L_5(\mathbf{r}_w(t))\gamma_b(t) \tag{12}$$

where L_4 is a shift operator that updates the indices of the wake vortices at each time step as a new wake vortex is shed from the trailing edge and L_5 denotes geometric operator that represents the induced velocity obtained form the Biot–Savart law.

The path of wake particles is determined using the Euler integration scheme; that is

$$(\mathbf{r}_w)_i(t+1) = (\mathbf{r}_w)_{i+1}(t) + \mathbf{u}_{w,i}((\mathbf{r}_w)_{i+1}(t), t)\Delta t \tag{13}$$

where $(\mathbf{r}_w)_i$ is the position of a given vortex in the wake and is calculated by convecting the downstream end point of segment $i-1$ found at previous time step and Δt is the time step. The velocity of the wake vortices $\mathbf{u}_w$ is then computed using the Biot–Savart law and combining the effects of the airfoil, the wake and the freestream on the wake. A major problem might occur in the system of point vortices when two vortices are convected close to each other. As such, the vortex blob concept is used to remove such singularity. More details of this concept are provided by Pettit et al. [12,17]. Equation (13) is then expressed as

$$\mathbf{r}_w(t+1) = L_6(\mathbf{r}_w(t))\gamma_w(t) + L_7(\mathbf{r}_w(t))\gamma_b(t) + L_8\mathbf{V}_\infty(t) \tag{14}$$

where L_6 and L_7 denote geometric operators that represent the induced velocity obtained form the Biot–Savart law and L_8 is an operator through which the fluctuations in the freestream velocity are applied on each wake vortex location. The governing equations of the UVLM including gust effects are given by Eqs. (8), (12), and (14). These equations are used in the implementation of the intrusive PCE.

C. Aerodynamic Lift

The computation of the aerodynamic lift is performed by multiplying the difference in the pressure across each panel by its length. These pressure differences are evaluated from the unsteady Bernoulli equation:

$$\frac{\partial\Phi_i}{\partial t} + \frac{p_i}{\rho} + \frac{1}{2}v_i^2 = H(t) \tag{15}$$

Rewriting Eq. (15) in terms of a differential between a control point i on the body and a point in the far field lying on the same streamline, the pressure coefficient $(Cp)_i = \frac{p_i - p_\infty}{\frac{1}{2}\rho V_\infty^2}$ is given by

$$(Cp)_i = 1 - \left(\frac{v_i}{V_\infty}\right)^2 - \frac{2}{V_\infty^2}\frac{\partial\Phi_i}{\partial t} \tag{16}$$

The difference in the pressure coefficient across each panel i of the plate is

$$\Delta(Cp)_i = \left[\left(\frac{v_i}{V_\infty}\right)_u^2 - \left(\frac{v_i}{V_\infty}\right)_l^2\right] + \frac{2}{V_\infty^2}\left[\left.\frac{\partial\Phi_i}{\partial t}\right|_u - \left.\frac{\partial\Phi_i}{\partial t}\right|_l\right] \tag{17}$$

where $(.)_u$ and $(.)_l$ stand for the upper and lower surfaces of the plate, respectively. For convenience, $(\frac{v_i}{V_\infty})$ will be replaced by v_i. The first term in Eq. (17) can be rewritten as

$$\begin{aligned}(v_i)_u^2 - (v_i)_l^2 &= ((v_i)_u + (v_i)_l)((v_i)_u - (v_i)_l) = 2(v_i)_m\Delta v_i \\ &= 2\cos(\alpha)\Delta v_i\end{aligned} \tag{18}$$

where α is the angle of attack. The velocity difference across a panel surface Δv_i is obtained by dividing the vorticity circulation strength $(\gamma_b)_i$ by the panel length $(\Delta l)_i$.

The calculation of the unsteady portion of Eq. (17) involves determining the rate of change of velocity potential Φ. The partial derivative is approximated through the first-order backward difference as

$$\frac{\partial\Phi}{\partial t} \approx \frac{\Phi(r,t) - \Phi(r, t-\Delta t)}{\Delta t} \tag{19}$$

Thus

$$\begin{aligned}\frac{2}{V_\infty^2}\left[\left.\frac{\partial\Phi_i}{\partial t}\right|_u - \left.\frac{\partial\Phi_i}{\partial t}\right|_l\right] &= \frac{2}{V_\infty^2\Delta t}[((\Phi_i)_u(t) - (\Phi_i)_l(t)) \\ &- ((\Phi_i)_u(t-\Delta t) - (\Phi_i)_l(t-\Delta t))]\end{aligned} \tag{20}$$

To calculate the difference in Φ across the panel surface in Eq. (20), the definition of the velocity potential, $v = \nabla\Phi$, is manipulated to state $\mathrm{d}\Phi = v\cdot\mathrm{d}l$ or

$$(\Phi)_u - (\Phi)_l = \int_{l_l}^{l_u} v\cdot\mathrm{d}l \tag{21}$$

Because the plate is considered as a body of zero thickness, the integration of Eq. (21) is performed along a closed path. Using the definition of circulation

$$\gamma = \oint_c v\cdot\mathrm{d}l \tag{22}$$

the value of the integral of Eq. (21) is equal to the circulation associated with the vorticity encircled by that path. In this formulation, the circulation is simply the summation of individual strengths of vortices encountered along the path of integration. Consequently, the difference in the velocity potential is given by

$$(\Phi_i)_u(t) - (\Phi_i)_l(t) = \sum_{j=1}^{i}(\gamma_b)_j(t) \tag{23}$$

The aerodynamic lift is then calculated by integrating the pressure over the entire plate as follows:

$$\begin{aligned}c_l(t) = \sum_{i=1}^{N}\Bigg[&2\cos(\alpha)\frac{(\gamma_b)_i(t)}{(\Delta l)_i} + \frac{2}{V_\infty^2\Delta t}\left(\sum_{j=1}^{i}(\gamma_b)_j(t)\right. \\ &\left.-\sum_{j=1}^{i}(\gamma_b)_j(t-\Delta t)\right)\Bigg]\Delta l\cos(\alpha)\end{aligned} \tag{24}$$

IV. Uncertainty Propagation

A. Spectral Representation of the Uncertainty

The spectral representation of uncertainty is based on the decomposition of the random function (or variable) into separable deterministic and stochastic components [18,19]. Thus, a random variable α^* is considered as a function of independent deterministic variables x and t and n-dimensional random variable vector $\xi = (\xi_{i_1}, \ldots, \xi_{i_n})$. It is expressed as

Table 1 Mean values and assumed standard deviations of the von Karman spectrum parameters

Parameter	Mean	Standard deviation
σ_u	1.716 ft/s	0.1716 ft/s
L_u	505.2 ft	50.50 ft
σ_v	1.000 ft/s	0.1000 ft/s
L_v	50.00 ft	5.000 ft

$$\alpha^*(x,t,\xi) = \sum_{m=0}^{\infty} \alpha_m(x,t)\Psi_m(\xi) \tag{25}$$

Here $\alpha_m(x,t)$ is the deterministic component, which is the amplitude of mth fluctuation, and $\Psi_m(\xi)$ is the random basis function corresponding to the mth mode. In practice, the finite-term summation should be limited by the highest order terms of the polynomials that yield the required accuracy. Many choices are possible for the basis functions depending on the type of the probability distribution selected for the uncertainty of the random variable vector ξ [20]. For variables with probability distributions that are Gaussian, Hermite polynomials are used because they form an orthogonal set of basis functions [21]. The Hermite polynomial of order n is defined as [21]

$$H_n(\xi_{i_1},\ldots,\xi_{i_n}) = e^{\frac{1}{2}\xi^T\xi}(-1)^n \frac{\partial^n}{\partial\xi_{i_1}\ldots\partial\xi_{i_n}} e^{-\frac{1}{2}\xi^T\xi} \tag{26}$$

For ξ being a standard Gaussian distributed variable, the inner product has the form

$$\langle\Psi_i(\xi),\Psi_j(\xi)\rangle = \frac{1}{\sqrt{(2\pi)^n}}\int_{-\infty}^{\infty}\cdots\int_{-\infty}^{\infty}\Psi_i(\xi)\Psi_j(\xi)e^{\left(-\frac{\xi^T\xi}{2}\right)}\,\mathrm{d}\xi \tag{27}$$

with the density function of the n variate standard Gaussian distribution as a weighting function.

B. Gust Uncertainties

For specified values of the spectral parameters (σ_u, L_u, σ_v and L_v), realizations for $u(t)$ and $v(t)$ are computed through Eqs. (1) and (2). Denoting the random vector composed of these parameters by Ξ and the corresponding random velocity components by $\mathbf{V}_\infty(t,\Xi) = [u_\infty(t,\Xi) = V_\infty + u(t,\Xi), v_\infty(t,\Xi)]^T$, this component is expanded as

$$\mathbf{V}_\infty(t,\Xi) = \sum_{m=0}^{P}\mathbf{V}_{\infty m}(t)\Psi_m(\Xi) \tag{28}$$

where $P+1 = \frac{(n+p)!}{n!p!}$ is the number of output modes, which is a function of the order of the polynomial chaos p and the number of random dimensions n. The coefficients $\mathbf{V}_{\infty m}(t) = [u_{\infty m}(t) = V_\infty + u_m(t), v_{\infty m}(t)]^T$ are determined from a nonintrusive PCE procedure, i.e., by 1) generating samples of the uncertain spectral parameters using Latin Hypercube sampling [22,23], 2) constructing the time histories for the gust velocities for each sample using Eqs. (1) and (2), and 3) using all samples to evaluate the PCE coefficients of the truncated expansion of $\mathbf{V}_\infty$ from

$$\mathbf{V}_{\infty m}(t) \approx \frac{\frac{1}{N}\sum_{n=1}^{N}\mathbf{V}_\infty(t,\xi_n)\Psi_m(\xi_n)}{\langle\Psi_m^2\rangle} \tag{29}$$

where $\xi_\lambda = (\lambda - \mu_\lambda)/\sigma_\lambda$ and $\lambda \in \{\sigma_v, L_v, \sigma_u, L_u\}$.

To generate the samples, variations of the spectral parameters are obtained by assuming Gaussian distributions with 10% coefficients of variation and mean values that are computed from the specifications in MIL-HDBK-1797 [11].

For a MAV with an assumed flight speed of 25 ft/s at an elevation of 100 ft, the mean and standard deviations of the integral length scales and intensities of the stochastic gust are presented in Table 1. It is noted that, based on the assumed ranges of gust parameters, the fluctuation levels should not cause notable leading-edge separation.

The PCE coefficients of $\mathbf{V}_\infty$ are determined using 200 realizations of turbulent velocity components. The zero- and first-order polynomial chaos coefficients are shown in Fig. 2. The zero-order coefficients are the estimated mean values of the stochastic gust. The first-order coefficients provide a measure of the sensitivity of the stochastic gust to each of the uncertain parameters ξ_1, ξ_2, ξ_3, and ξ_4 which correspond to the spectral parameters σ_v, L_v, σ_u, and L_u, respectively. These coefficients are the inputs of the stochastic version of the UVLM as will be shown in the following subsection. It should be noted that the time histories of the unsteady wind velocities are computed for a total physical time of 2 s on a flat-plate airfoil with a chord of 0.5 ft. These parameters were chosen to ensure the inclusion of all gust wavelengths that cannot be modeled using quasi-steady aerodynamics.

C. Intrusive Formulation

In the intrusive approach, spectral decomposition of the flow parameters, as described in the previous section, is introduced in the governing equations. In implementing the intrusive approach for the current work, the strengths of the bound and wake vortex elements for the fixed airfoil with wake vortex convection, $\gamma_b(t,\xi)$ and $\gamma_w(t,\xi)$, are considered as stochastic processes that are functions of the statistics of the upstream gust. Their PCE are then written as

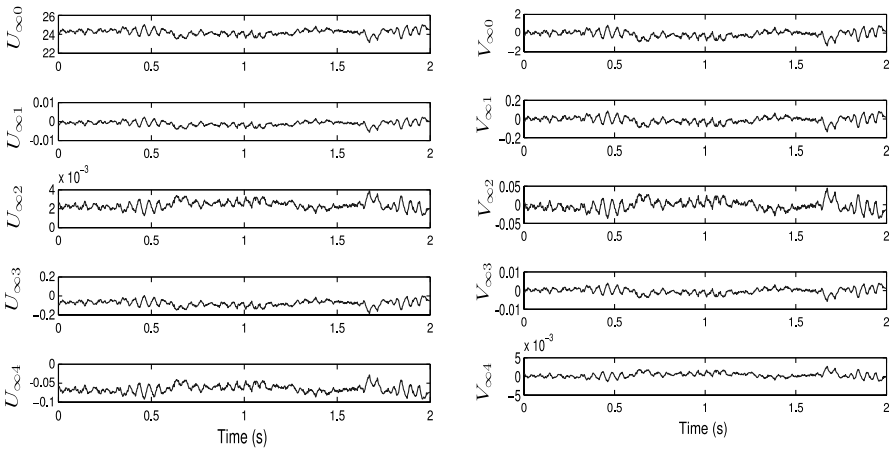

a) $U_{\infty m}(t)$ **b)** $V_{\infty m}(t)$

Fig. 2 The PCE coefficients of the components of the random freestream flow speed. The zero-order coefficients are the estimated mean values of the stochastic gust. The first-order coefficient provide a measure of the sensitivity of the stochastic gust to each of the uncertain parameters.

$$\gamma_b(t,\Xi)=\sum_{m=0}^{P}\gamma_{bm}(t)\Psi_m(\Xi) \tag{30a}$$

and

$$\gamma_w(t,\Xi)=\sum_{m=0}^{P}\gamma_{wm}(t)\Psi_m(\Xi) \tag{30b}$$

For the sake of simplicity, the wake elements locations, $\mathbf{r}_w(t)$, are considered to be deterministic. The basis of this assumption is the result that ignoring effects of minor stochastic variations in the positions $\mathbf{r}_w(t)$ of the wake vortices does not significantly influence the airfoil loads [17].

The intrusive approach relies on a Galerkin projection of the original model equations to arrive at governing equations for the PC mode strengths of the model output [7,21]. The governing equations are rewritten by substituting Eqs. (28) and (30) in Eqs. (8), (12), and (14), that is

$$\begin{aligned}
&L_1\sum_{m=0}^{P}\gamma_{bm}(t)\Psi_m(\xi)=L_2(\mathbf{r}_w(t))\sum_{m=0}^{P}\gamma_{wm}(t)\Psi_m(\xi)\\
&\quad+L_3\sum_{m=0}^{P}\mathbf{V}_{\infty m}\Psi_m(\xi)\\
&\sum_{m=0}^{P}\gamma_{wm}(t+1)\Psi_m(\xi)=L_4\sum_{m=0}^{P}\gamma_{wm}(t)\Psi_m(\xi)\\
&\quad+L_5(\mathbf{r}_w(t))\sum_{m=0}^{P}\gamma_{bm}(t)\Psi_m(\xi)\\
&\mathbf{r}_w(t+1)=L_6(\mathbf{r}_w(t))\sum_{m=0}^{P}\gamma_{wm}\Psi_m(\xi)+L_7(\mathbf{r}_w(t))\sum_{m=0}^{P}\gamma_{bm}\Psi_m(\xi)\\
&\quad+L_8\sum_{m=0}^{P}\mathbf{V}_{\infty m}\Psi_m(\xi)
\end{aligned} \tag{31}$$

Based on the orthogonality of the basis functions (Hermite polynomials), projecting Eq. (31) onto $\{\Psi_l(\xi)\}$ yields the stochastic version of the UVLM governing equations

$$\begin{aligned}
&L_1\gamma_{bl}(t)=L_2(\mathbf{r}_w(t))\gamma_{wl}(t)+L_3\mathbf{V}_{\infty l}(t),\quad (l=0,1,\ldots,P)\\
&\gamma_{wl}(t+1)=L_4\gamma_{wl}(t)+L_5(\mathbf{r}_w(t))\gamma_{bl}(t)\\
&\quad(l=0,1,\ldots,P),\ \text{and}\\
&\mathbf{r}_w(t+1)=L_6(\mathbf{r}_w(t))\gamma_{w0}(t)+L_7(\mathbf{r}_w(t))\gamma_{b0}(t)+L_8\mathbf{V}_{\infty 0}(t)
\end{aligned} \tag{32}$$

The above system of $(2P+3)$ equations is solved at each time step for the PCE coefficients γ_{bl} and γ_{wl}. The inputs are the PCE coefficients of the freestream flow speed $\mathbf{V}_{\infty m}(t)=[u_{\infty m}(t)=V_\infty+u_m(t), v_{\infty m}(t)]^T$ and the initial conditions at $t=0$ that are $\gamma_w(0)=0$ and $\mathbf{r}_w(0)=0$ because no wake vortices exist yet. Note that, at each time step, a new vortex is shed from the airfoil's trailing edge, as in the deterministic UVLM.

V. Results and Discussion

A. Global Sensitivity Analysis

Considering the unsteady lift coefficient, $c_l(t,\xi)$ as a stochastic quantity, it is approximated by a truncated polynomial expansion of the form

$$c_l(t,\Xi)=\sum_{m=0}^{P}c_{l_m}(t)\Psi_m(\Xi) \tag{33}$$

Substituting Eqs. (30a) and (33) into Eq. (24), projecting the resulting equations onto $\Psi_m(\xi)$, we obtain the PCE coefficients of $c_l(t,\xi)$ given by the following:

$$\begin{aligned}
c_{l_m}(t)=\sum_{i=1}^{N}\Bigg[&2\cos(\alpha)\frac{(\gamma_{bm})_i(t)}{(\Delta l)_i}+\frac{2}{V_\infty^2\Delta t}\Bigg(\sum_{j=1}^{i}(\gamma_{bm})_j(t)\\
&-\sum_{j=1}^{i}(\gamma_{bm})_j(t-\Delta t)\Bigg)\Bigg]\Delta l\cos(\alpha)
\end{aligned} \tag{34}$$

The computation of the PCE coefficients presents several advantages over performing a statistical analysis of the output data. In particular, the first-order terms in these coefficients provide a measure of the sensitivity of the stochastic process to each of the uncertain parameters. Figure 3 depicts the time histories of the zero-order polynomial chaos coefficient c_{l_0} and the first-order coefficients c_{l_1} through c_{l_4}. The zeroth-order term is the estimated ensemble mean value of the stochastic process, $c_l(t,\xi)$. The first-order terms are the estimated linear coefficients for $\Psi_1=\xi_1$ through $\Psi_4=\xi_4$, which correspond to σ_v, L_v, σ_u and L_u, respectively. The relative importance of the linear dependence of the response on ξ_1 through ξ_4 can be inferred from relative magnitudes of these coefficients. Obviously, the magnitudes of c_{l_2}, c_{l_3}, and c_{l_4} are much smaller than that of c_{l_1}. This indicates that the $c_l(t)$ fluctuations are most sensitive to imprecision in the intensity of the vertical turbulence component σ_v. Then, in order of importance, the next is the imprecision in L_v which is the integral length scale of the vertical turbulence.

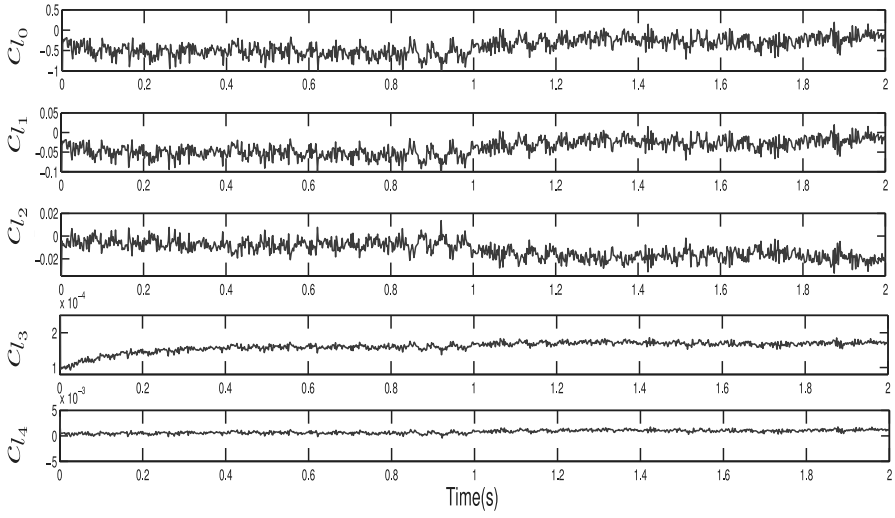

Fig. 3 Time histories of the zeroth-order polynomial chaos coefficient, c_{l_0}, and the first-order coefficients, c_{l_1} through c_{l_4}, for the lift coefficient due to atmospheric turbulence.

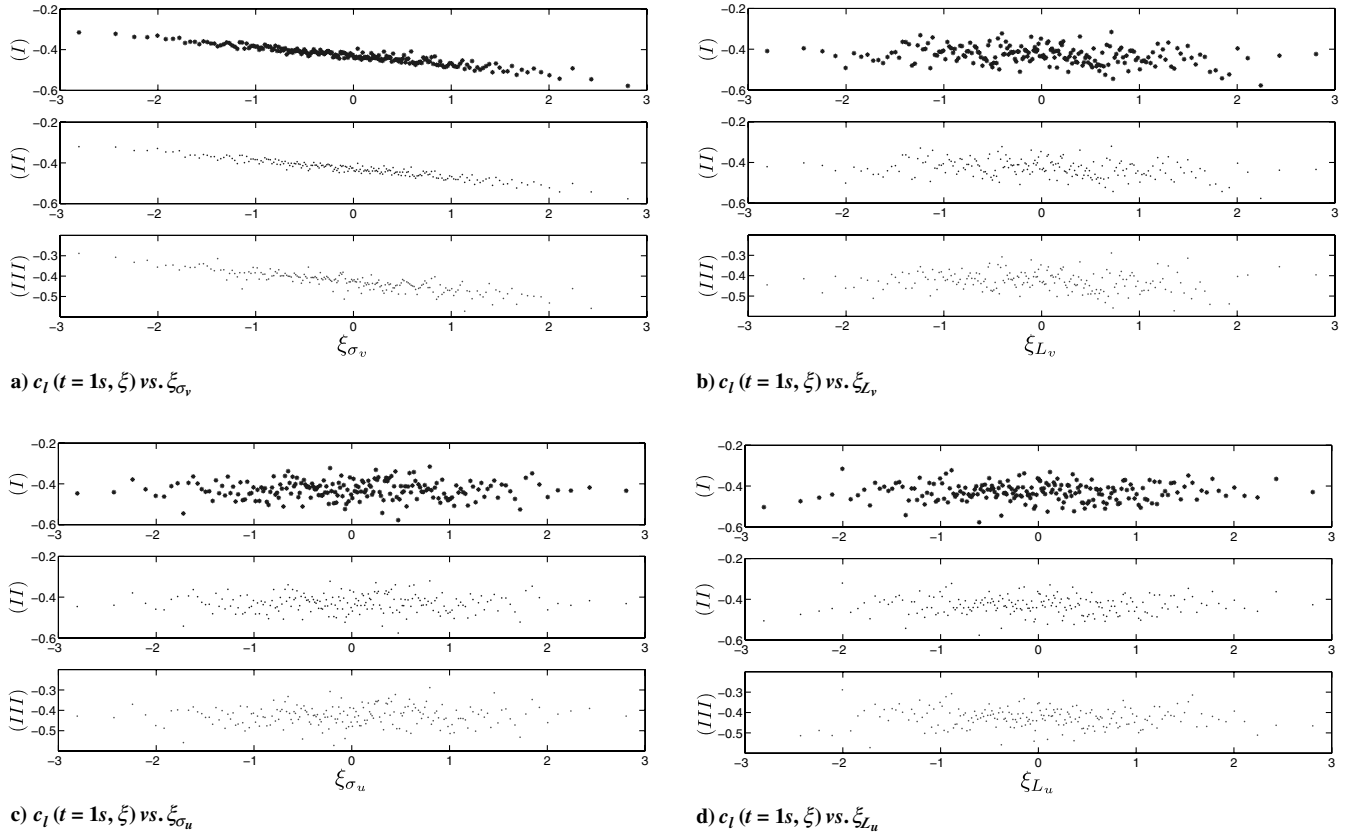

a) $c_l\,(t = 1s, \xi)\ vs.\ \xi_{\sigma_v}$ **b)** $c_l\,(t = 1s, \xi)\ vs.\ \xi_{L_v}$

c) $c_l\,(t = 1s, \xi)\ vs.\ \xi_{\sigma_u}$ **d)** $c_l\,(t = 1s, \xi)\ vs.\ \xi_{L_u}$

Fig. 4 Lift coefficient at $t = 1$ s versus ξ_i. In each part of the figure, (I) depicts the original data, and (II) and (III) show the same data simulated by the first-order and second-order PCE, respectively. The results are plotted separately for ease of comparison.

B. Validation

The sensitivity to each of the four random parameters can also be determined from the response at a given time as a function of each Ξ component. To this end, 200 realizations of lift coefficients were generated using the same uncertain spectral parameters of the generated flow field in the intrusive formulation. Variations of the lift coefficient with different ξ_i at $t = 1.0$ s are plotted in Fig. 4. The upper plots (I) present variations obtained from the 200 LHS realizations. The lower plots (II) and (III) show variations obtained from the first-order and second-order intrusive PCE formulations, respectively. A linear regression analysis of the data in (I) plots is performed to determine the effectiveness of the intrusive PCE in measuring the first-order sensitivity to assumed randomness in the gust model's parameters. A comparison between the slopes obtained from the regression analysis and the corresponding PCE coefficient at $t = 1$ s is presented in Table 2. This comparison shows that the 1st-order intrusive PCE produces coefficients that accurately represent the first-order sensitivity of the lift coefficient to imprecision in gust spectra. The second-order intrusive PCE produces coefficients that are relatively less accurate than their first-order counterparts. Clearly, only linear expansion terms are required in the PC expansion and the inclusion of the nonlinear or cross-terms in the expansion leads to small errors in the estimated lift coefficient. Furthermore, the higher slope of c_l vs ξ_{σ_v} is consistent with the expectation that the variations in the lift coefficient are linearly related to variations in the fluctuations of the vertical turbulence component.

To analyze the statistics of the MC and intrusive PC methods quantitatively, we consider the stochastic aerodynamic lift at 4 times ($t = 0.5$, 1, 1.5, and 2 s). Figure 5 shows empirical density functions of the lift coefficient at these times. The density functions are computed from 200 realizations based on both the original time histories (from the deterministic model) and those determined from the first- and second-order intrusive PCE. The results show an excellent match between the data obtained from the MC and first-order PCE. The PDF of the aerodynamic lift is nearly Gaussian when obtained from the MC and 1st-order PCE but non-Gaussian and slightly skewed to the right when the 2nd-order PCE terms are included.

The mean and standard deviation values of the stochastic aerodynamic lift obtained from the MC simulations combined with LHS as well as the intrusive PC methods are presented in Table 3. For the second-order PCE, the mean and standard deviations values are slightly different from those obtained with MC simulations, whereas, the first-order accurately yield the statistics of the stochastic aerodynamic lift. The results show that including quadratic terms in the PCE expansion cause errors in the estimation of the bound and wake vorticity circulation. In fact, the intrusive PCE is exact in an analytical sense, but the use of a nonintrusive PCE for $\mathbf{V}_\infty$ causes

Table 2 Comparison between the slope obtained from the regression analysis and the corresponding PCE coefficient at $t = 1.0$ s. The 95% confidence intervals for the slopes are calculated for Monte Carlo simulations using the Bootstrap method

	MC	First-order PCE	Second-order PCE	95% Conf. Interval
c_l vs ξ_{σ_v}	-0.0427	-0.0425	-0.0467	$[-0.0428, -0.0427]$
c_l vs ξ_{L_v}	-0.0121	-0.0120	-0.0130	$[-0.0121, -0.0118]$
c_l vs ξ_{σ_u}	1.66×10^{-4}	1.65×10^{-4}	2.70×10^{-4}	$[0.612 \times 10^{-4}, 3.485 \times 10^{-4}]$
c_l vs ξ_{L_u}	7.96×10^{-4}	7.91×10^{-4}	3.28×10^{-3}	$[7 \times 10^{-4}, 11 \times 10^{-4}]$

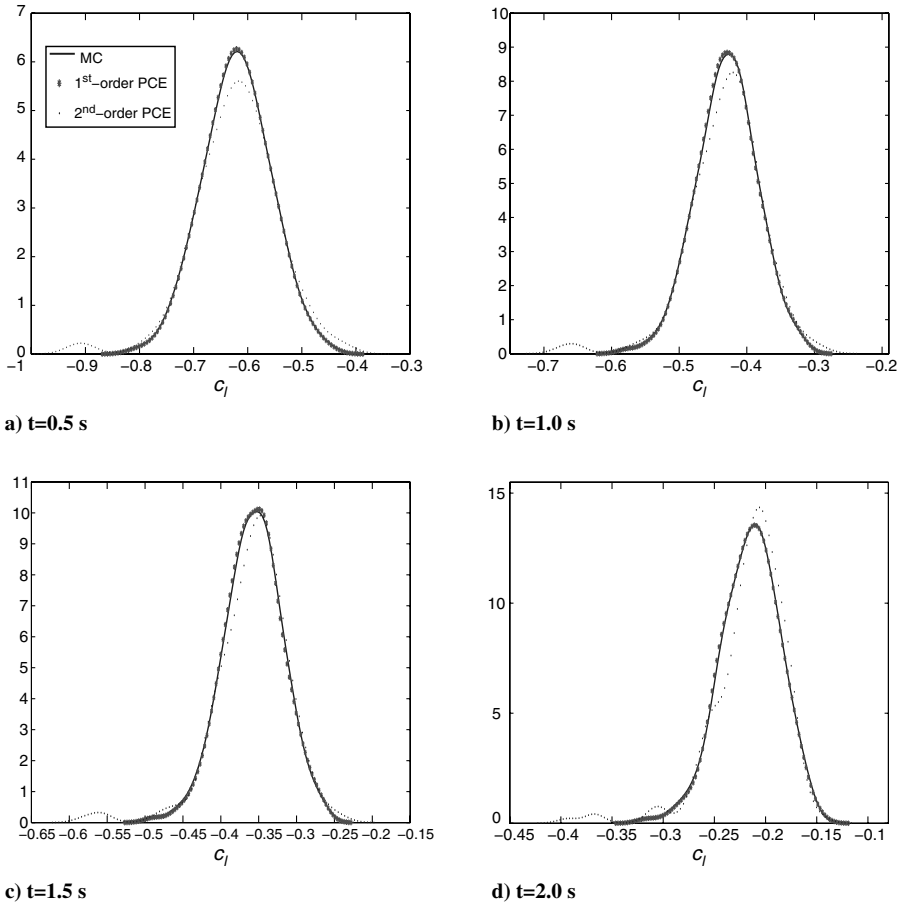

Fig. 5 Empirical density functions for c_l at $t = 0.5$, 1.0, 1.5, and 2.0 s. The solid blue lines is the estimated density function from the original time histories. The dashed red and blue line represent the estimated density function from the first-order and second-order PCE, respectively.

Table 3 The mean and standard deviation of the lift coefficient c_l obtained with intrusive PCE and MC combined with LHS

		MC	First-order PCE	Second-order PCE
$t = 0.5$ s	Mean	−0.620	−0.620	−0.621
	StD	0.062	0.0616	0.0765
$t = 1$ s	Mean	−0.429	−0.429	−0.430
	StD	0.0444	0.0441	0.0552
$t = 1.5$ s	Mean	−0.357	−0.357	−0.358
	StD	0.0383	0.038	0.0477
$t = 2$ s	Mean	−0.215	−0.215	−0.216
	StD	0.0283	0.0280	0.0351

statistical estimation errors that corrupt the second-order terms and presumably the higher-order terms.

VI. Conclusions

The intrusive polynomial chaos approach was implemented to determine uncertainty in gust loads on a rigid airfoil due to imprecision in an incoming gust characteristics. The results yield the sensitivity of the lift coefficient, $c_l(t)$, to variations in the intensities and integral length scales of the gust fluctuations. Lift coefficient fluctuations about the mean at each time step were affected primarily by the intensity of the vertical fluctuations σ_v, which should be expected for an airfoil fixed at zero angle of attack. Second in order of importance was the integral length scale of the vertical velocity component, L_v. As might be expected, $c_l(t)$ was relatively insensitive to the streamwise gust parameters. Consequently, if the flow model and parameter ranges employed here are appropriate of the intended application, a stochastic analysis of the effects of gust on the lift coefficient of an airfoil would be satisfactory if the streamwise gusts were neglected. More generally, the analysis presented here provides a basis for exploring these and other parametric effects in a broad range of gust loads analyses. This successful implementation of the intrusive PCE provides guidance and a baseline for efforts to quantify uncertain gust loads on MAVs with higher fidelity models.

Acknowledgment

Support by Air Force Research Laboratory Contract FA 8650-09-02-3938 is acknowledged.

References

[1] Tieleman, H. W., Ge, Z., Hajj, M. R., and Reinhold, T. A., "Wind Tunnel Simulation of Time Variations of Turbulence and Effects on Pressure on Surface-Mounted Prisms," *Journal of Wind Engineering and Industrial Aerodynamics*, Vol. 88, Nos. 2–3, 2000, pp. 197–212.

[2] Tieleman, H. W., "Universality of Velocity Spectra," *Journal of Wind Engineering and Industrial Aerodynamics*, Vol. 56, No. 1, 1995, pp. 55–69. doi:10.1016/0167-6105(94)00011-2

[3] Pagnini, L. C., and Solari, G., "Gust Buffeting and Turbulence Uncertainties," *Journal of Wind Engineering and Industrial Aerodynamics*, Vol. 90, Nos. 4–5, 2002, pp. 441–159.

[4] Saltelli, A., Chan, K., and Scott, E. M., (eds.), *Sensitivity Analysis*, Wiley, New York, 2000.

[5] Saltelli, A., *Global Sensitivity Analysis: The Primer*, John Wiley, Chichester, England, 2008.

[6] Pettit, C. L., "Uncertainty Quantification in Aeroelasticity: Recent Results and Research Challenges," *Journal of Aircraft*, Vol. 41, No. 5, Sep.–Oct. 2004, pp. 1217–1229. doi:10.2514/1.3961

[7] Najm, H. N., "Uncertainty Quantification and Polynomial Chaos Techniques in Computaional Fluid Dynamics," *Annual Review of Fluid Mechanics*, Vol. 41, 2009, pp. 35–52.

[8] Tennekes, H., and Lumley, J., *A First Course in Turbulence*, The MIT

Press, Cambridge, MA, 1972.
[9] Frisch, U., *Turbulence: The Legacy of A, N. Kolmogorov*, Cambridge Univ. Press, Cambridge, England, 1995.
[10] Hoblit, F. M., *Gust Loads on Aircraft: Concepts and Applications*, AIAA Education Series, AIAA, Washington, D.C., 1988.
[11] MIL, U.S. Military Handbook MIL-HDBK-1797, 1997.
[12] Pettit, C. L., Hajj, M. R., and Beran, P. S., "A Stochastic Approach for Modeling Incident Gust Effects on Flow Quantities," *Probabilistic Engineering Mechanics*, Vol. 25, No. 1, 2010, pp. 153–162. doi:10.1016/j.probengmech.2009.08.007
[13] Paola, M. D., "Digital Simulation of Wind Field velocity," *Journal of Wind Engineering and Industrial Aerodynamics*, Vol. , Nos. 1–2, 1998, pp. 91–109. doi:10.1016/S0167-6105(98)00008-7
[14] Grigoriu, M., *Stochastic Calculus: Applications in Science and Engineering*, Cambridge Univ. Press, Cambridge, England, 2002.
[15] DeLaurier, J., and Winfield, J., "Simple Marching-Vortex Model for Two-Dimensional Unsteady Aerodynamics," *Journal of Aircraft*, Vol. 27, No. 4, 1990, pp. 376–378. doi:10.2514/3.25282
[16] Wang, Z., "Time-Domain Simulations of Aerodynamic Forces on Three-Dimensional Configurations, Unstable Aeroelastic Responses, and Control by Network Systems," Ph.D. Thesis, Virginia Polytechnic Inst. and State Univ., Blacksburg, VA, 2004.
[17] Pettit, C., Hajj, M. R., and Beran, P. S., "Gust Loads with Uncertainty Due to Imprecise Gust Velocity Spectra," *48th AIAA/ASME/ASCE/AHS/ASC Structures, Structural Dynamics, and Materials Conference*, AIAA Paper 2007-1965, Reston, VA, 2007.
[18] Reagan, M., Najm, H. N., Ghanem, R. G., and Knio, O. M., "Uncertainty Quantification in Reacting Flow Simulations Through Non-Intrusive Spectral Projection," *Combustion and Flame*, Vol. 132, No. 3, 2003, pp. 545–555. doi:10.1016/S0010-2180(02)00503-5
[19] Hosder, S., Walters, R. W., and Rafael, P., "A Non-Intrusive Polynomial Chaos Method for Uncertainty Propagation in CFD Simulations," *44th AIAA Aerospace Sciences Meeting and Exhibit*, AIAA Paper 2006-891, Reno, Nevada, 2006.
[20] Xiu, D., and Karniadakis, G. E., "Modeling Uncertainty in Flow Simulations via Generalized Polynomial Chaos," *Journal of Computational Physics*, Vol. 187, No. 1, 2003, pp. 137–167. doi:10.1016/S0021-9991(03)00092-5
[21] Ghanem, R., and Spanos, P. D., *Stochastic Finite Elements: A Spectral Approach*, Dover Publications, Inc., New York, 2003.
[22] Helton, J. C., and Davis, F. J., "Sampling-Based Methods," edited by A. Saltelli, K. Chan, and M. Scott, Wiley, New York, Chap. 6.
[23] Helton, J. C., and Davis, F. J., "Latin Hypercube Sampling and the Propagation of Uncertainty in Analyses of Complex Systems," *Reliability Engineering and System Safety*, Vol. 81, No. 1, 2003, pp. 23–69.